Available online at www.sciencedirect.com
SCIENCE DIRECT
Optics Communications 263 (2006) 239–248
OPTICS COMMUNICATIONS
www.elsevier.com/locate/optcom

A self-consistent model for a SOA-based fiber ring laser including the mode-locked pulse properties

Vasilios Zarikas [a], Kyriakos Vlachos [b,*]

[a] Institute of Continuous Education, Aharnon 426, 111 43 Athens, Greece
[b] Research Academic Computer Technology Institute and Computer Engineering and Informatics Department, University of Patras, GR26500, Rio, Patra, Greece

Received 16 May 2005; received in revised form 10 November 2005; accepted 13 January 2006

Abstract

In this paper, we present a self-consistent model of an optically mode-locked semiconductor fiber ring laser. The fiber laser uses a semiconductor optical amplifier (SOA) as the gain medium, while mode-locking is achieved by its gain modulation, via an external optical pulsed signal. We solved the model analytically developing a novel technique, where we have assumed double saturation of the SOA by both the mode-locked and the externally introduced pulsed signal. The study revealed the locus of the laser parameters to achieve mode-locking. In particular, it was found that SOA gain and energy of the externally introduced signal are two critical parameters that must simultaneously set properly for exact mode-locking. Another outcome of our analysis is that the study of the chirp parameter should be carried out keeping the nonlinear terms of the SOA gain. We have also investigated a slightly detuning regime of operation that revealed a fast change of the mode-locking process.

Keywords: Mode-locking; Semiconductor optical amplifier; Ring laser; Optical gain modulation

1. Introduction

Optical sources capable of generating ultra-short pulse trains at high repetition rates [1–3] are key elements for high speed networks that combine WDM and OTDM transmission techniques. Active mode-locking is one of the key techniques for the generation of ultra-short, transform-limited optical pulses and is achieved by the direct modulation of the optical field during each laser cavity round-trip [4,5]. This method is particularly important especially when synchronization between optical and electrical signals is required. At 1.5 μm spectral window, several actively mode-locked fiber lasers employing erbium-doped fiber as the gain medium and producing transform-limited picosecond pulses at multi-GHz rates have been demonstrated [6–16]. The majority of these systems use loss modulation by lithium niobate electro-optic modulators due to their large electro-optic coefficient and their compact construction on low loss titanium-undiffused waveguides. Unfortunately, lithium niobate modulators are polarization sensitive devices and as a result, laser sources using lithium niobate modulators either have to be build from polarization preserving fiber pigtailed components [13–15] or with complex stabilization feedback circuits [16–19] or incorporating high-finesse FP filters [20,21]. Active stabilization techniques have been developed to continuously monitor and correct the driving frequency or cavity length for countering the tendency towards instability of long cavity fiber lasers.

A very promising technique of active mode-locking has been demonstrated with intracavity SOAs to provide both gain and modulation in the cavity with the additional advantage that mode-locking can be achieved via XGM modulation from an external optical signal. In particular, actively mode-locked laser sources, incorporating SOAs, have been

* Corresponding author. Tel.: +30 2610 996990; fax: +30 210 7018178.
E-mail address: kvlachos@ceid.upatras.gr (K. Vlachos).

0030-4018/$ - see front matter © 2006 Elsevier B.V. All rights reserved.
doi:10.1016/j.optcom.2006.01.016

demonstrated by several research groups [22–26] for the generation of short optical pulses at various repetition rates. In these experiments, the SOA was used either as the gain or as the modulation element in the cavity in combination with an additional intracavity intensity modulator [9,23,24] or used to provide both gain and electrically controlled gain modulation [25]. Additionally, SOAs have been also used as the mode-locking elements providing gain modulation in Er-doped fiber ring lasers or storage rings [26,27].

In this paper, we present for the first time an accurate self-consistent model of a novel SOA-based fiber laser. The laser has been used for short picosecond pulsetrains generation either under single-wavelength or multiwavelength operation mode. It uses a single active element, a SOA, to provide both gain and gain modulation in a fiber cavity via cross-gain saturation from an external optical pulse train. This ring laser platform was first demonstrated at 10 GHz [28] and was extended to 40 GHz single-wavelength operation [29,30] and 30 GHz multi-wavelength operation [31–33] exploiting further the nonlinear interaction of the optical pulses in the semiconductor. The use of a single SOA in the optical cavity in combination with the optical gain modulation yields significant performance advantages, as for example, the ultrafast modulation function, due to the fast carrier depletion of the SOA [30], the broad wavelength tunability [31], and the short picosecond pulse generation due to the nonlinear interaction of the optical signals in the SOA [34].

For modeling the SOA-based laser platform, we developed a self-consistent model, taking into account the mode-locked pulse properties and in particular the mode-locked pulse duration and energy in the SOA gain saturation profile. Albeit, it has been shown, [31–34], that the energy of the mode-locked pulsetrain is high enough to saturate the SOA, this has not been taken into account in other developed analytical models. To this end, in the model presented here, it is assumed that SOA is being saturated by both the externally introduced optical pulsetrain as well as from the re-circulating, mode-locked one. The analysis proved very complex due to the phase inclusion in the pulse profile and the nonlinearity of the SOA gain. Our study revealed a unique locus of the laser parameters to achieve mode-locking. In particular, it was found that SOA gain and energy of the externally introduced signal are two critical parameters that must simultaneously set properly for exact mode-locking. Other models developed for the same platform, cannot be applied without including phase changes in the model [35] or including loss modulation as against to gain modulation [36]. A more recent work presented in [37] takes into account phase variations but linearize SOA gain and assumes expansion of the exponentials in the master equation, resulting in a very simplified model. However, all works presented up to date, disregard the energy of the mode-locked pulse that may result in significantly different results.

Furthermore, in this paper, the laser operation under a slight cavity detuning is investigated. Studying an operation regime close to the optimum is important, primarily because it may reveal strong dependencies of various parameters and in general the system under study may exhibit a completely different behavior.

The rest of paper is organized as follows. Section 2 presents the principle of operation of the ring laser and the theoretical equations that govern its principles modules. Section 3 presents the laser self-consistent model, while Section 4 presents in detail the effect of the various physical parameters on the laser performance.

2. Laser and model description

2.1. Experimental configuration

Active mode-locking is a well-known technique that is widely used to generate ultra-short optical pulses at high repetition rates. It is achieved by modulating the loss, the gain or the phase of a laser. The theoretical treatment of active mode-locking in the time domain is generally based on the "self-consistent profile" method, developed by Siegman and Kuizenga [38,39] and Haus [40,41]. Comprehensive descriptions of the pulse formation process in various actively mode-locked lasers can be found in a number of studies. The basic approach is based upon the consideration of a ring laser configuration containing a gain medium and a modulator, with a signal that propagates in one direction through the laser. The laser can also incorporate various additional components that affect the signal. It is assumed that an optical pulse has formed so that after a large number of round-trips, the electrical field E can be described as:

$$E_{\text{pulse}}(t) = k \exp\left[-\frac{1+\mathrm{i}\theta}{2}\left(\frac{t}{\Delta T}\right)^2\right] \tag{1}$$

where θ is the chirp parameter. In our model, we have used a Gaussian pulse shape. This is a fair approximation. However, a super Gaussian pulse can also be used to solve the steady-state equations following our proposed in the present paper, step method, keeping the right order terms of the integrated gain function. In our setup the Gaussian shape suffices for the theoretical modeling. For simplicity we define:

$$k = \sqrt{\frac{U_0 E_{\text{sat}}}{\Delta T}} \tag{2}$$

and thus the pulse power is

$$p_{\text{in}}(t) = k^2 \exp\left[-\frac{1}{2}\left(\frac{t}{2\Delta T}\right)^2\right] \tag{3}$$

U_0 is the input pulse energy, normalized to the saturation energy E_{sat} and the pulse width.

The inclusion of a phase in our model is necessary for an accurate description of the experiment. The appearance of a phase is due to the known as SPM, self-phase modulation phenomenon. SOA gain saturation leads to a depletion of the carrier density which in turn results to nonlinear

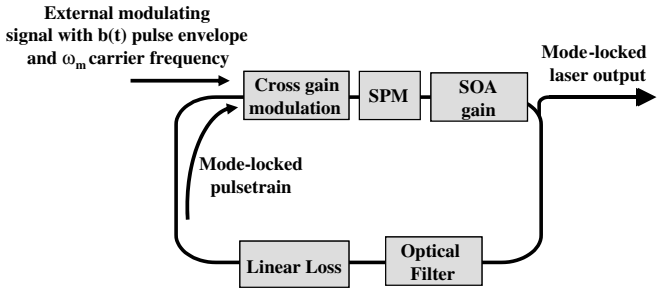

Fig. 1. Schematic diagram of the ring resonator used in the self-consistent profile model of active mode-locking.

changes in the refractive index. A careful theoretical study of the produced chirp and spectral broadening is important for achieving short and high-power pulse trains. Fig. 1 shows a schematic diagram of the SOA-based ring laser with the corresponding effects depicted.

In the absence of gain modulation and provided that the SOA gain exceeds the total cavity loss, the laser generates CW-radiation. The noise that oscillates in the cavity gradually develops to CW-light under the interplay of the amplifier and the filter. In actively mode-locked fiber lasers, the fundamental cavity frequency f_r is generally much smaller than the repetition frequency at which the laser is mode-locked. When the cavity includes a modulator driven at a frequency f_{ext} equal to an integer multiple of f_r, the laser is harmonically mode-locked:

$$f_{ext} \approx m f_r = m \frac{1}{T_r} = m \frac{c}{n_g l} \tag{4}$$

where m is an integer, T_r is the cavity round-trip time, l is the cavity length, c is the speed of light and n_g is the cavity group index. The number of pulses oscillating in the cavity equals m.

The principle of operation and repetition-frequency multiplication in our circuit relies on two key factors. The first is that the fast saturation of the gain of a semiconductor optical amplifier (SOA) by an externally introduced, optical pulsed signal is used for gain modulation in a fiber ring laser and for the generation of stable mode-locked picosecond pulses. In this instance the externally introduced optical pulse and the comparatively slow gain recovery of the SOA define a short temporal gain window within which the mode-locked pulse is formed.

The second key factor is that by detuning the frequency f_{ext} of the externally introduced pulse train to $f_{ext} = (m + 1/n)f_r$, one may obtain an output pulse train at a frequency $n \cdot f_{ext}$, where m is the order of harmonic mode locking of the ring laser and n is an integer number greater than 1. To this end, when the repetition rate of the external pulse train is adjusted to differ by f_r/n from a harmonic of the fundamental of the ring cavity, the mode-locked pulse becomes temporally displaced by T_{ext}/n on each recirculation through the ring cavity with respect to its previous position. T_{ext} is the repetition period of the external signal.

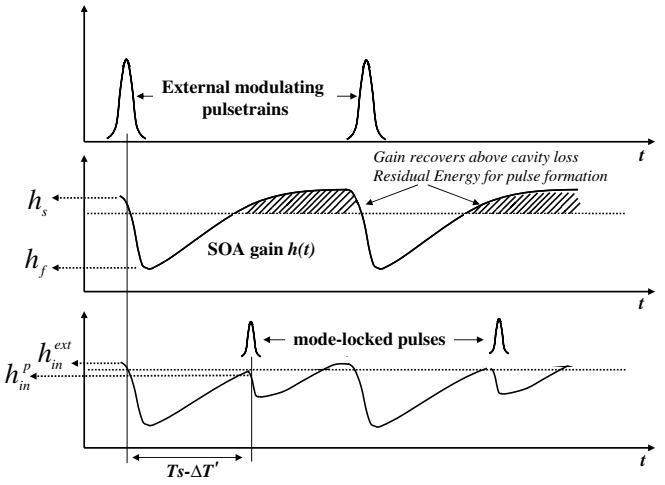

Fig. 2. Mode external optical pulse. The top figure shows the externally introduced pulses that modulate SOA gain at f_{ext} frequency. The middle figure displays the SOA gain curve. In particular, the horizontal dotted line in the gain curve indicate the loss line above which the net gain is positive enabling the formation of mode-locked pulses. In the middle figure, we denote by h_s and h_f the instant SOA gain before and after the external pulse transition. The bottom figure displays the formed mode-locked pulses, which are temporally displaced by $T_s - \Delta T'$ and the resulting SOA gain curve. The SOA gain is saturated by the mode-locked pulse, resulting in a different equilibrium state. In the bottom figure we denote by h_{in}^{p} and h_{in}^{ext} the instant SOA gain before the transition of the mode-locked and the external pulse respectively.

Fig. 2 illustrates graphically the mode-locking process based on the SOA gain modulation by an external pulse. The mode-locked pulse is formed, after the insertion of the external pulse, at the time that the slowly recovering gain of the SOA balances the cavity losses, denoted by the horizontal dotted line in Fig. 2. As the mode-locked pulse transits the SOA, its gain depletes again below the loss line, to recover slowly before the next external or mode-lock pulse enters it. This mechanism results in a temporal displacement between the external and mode-locked pulses in the SOA, denoted as $T_s - \Delta T'$. With respect to the multiplication process, the mode-locked pulses after n times re-circulations, are on average equally amplifies due to the temporal displacement, resulting in no pulse-to-pulse pattern distortion. An illustrated figure of the multiplication process can be found in [29]. The most important parameters that are crucial in the formation of the mode-locked pulse for any repetition frequency are mainly the cavity loss, the pulsewidth, average power of the external pulsetrain and the small signal gain of the SOA.

2.2. Laser model

In the self-consistent model described in the following section, we assume that each pulse in the ring laser employs the same properties, such that we may consider the propagation of a single pulse through the cavity. Each element of the ring laser in Fig. 1 is described by an operator. In steady-state operation, a re-circulating pulse satisfies the following operator equation:

$$E_{\text{out}} = \widehat{T}_3\widehat{T}_2\widehat{T}_1 E_{\text{pulse}} \tag{5}$$

Note that in the model developed we did not take into account the cavity dispersion primarily because this is negligible due to the short cavity length. Summarizing the model setup, the operators that hit the pulse are:

Filter: $\widehat{T}_1 = T_{\text{filter}}(\omega)$ in the frequency domain.
SOA: $\widehat{T}_2 = \mathrm{e}^{\frac{h(t)(1+\mathrm{i}\alpha)}{2}}$ in the time domain.
Linear loss: $\widehat{T}_3 = T_{\text{loss}}$.

In this study, we make no assumption for the operators of Eq. (5). Therefore in the steady-state equation, we do not expand the exponential terms in Taylor series, since this does not constitute a good approximation. Furthermore, it is useful to define the following time intervals:

t_1 is the time pulse needs to pass through the filter;
t_2 is the time pulse needs to travel from the exit of the filter to the entrance of the SOA;
t_3 is the time pulse needs travel from the exit of the SOA to the entrance of filter. It is obvious that $t_3 \approx$ optical length/c.

Thus, the time duration of a cavity round trip is:

$$T_{\text{r}} = t_1 + t_2 + t_3 \tag{6}$$

The proposed SOA-based ring is harmonically mode-locked, see Eq. (4), up to a detuning small time interval δT, following the period of the external pulse T_{ext}. Therefore:

$$T_{\text{r}} + \delta T = mT_{\text{ext}} \tag{7}$$

Following, we present the detailed expression of the operators used.

2.2.1. Optical filter

In our model, we have assumed a Gaussian filter with a frequency domain transfer function given by:

$$T_{\text{filter}}(\omega) = \exp\left[-\frac{(\omega-\delta\omega)^2}{2\Delta\omega_{\text{g}}^2}\right] \tag{8}$$

where the optical filter bandwidth is

$$\Delta\omega_{\text{g}} = \frac{1}{2\sqrt{\ln 2}}\Delta\omega_{\text{FWHM}} \tag{9}$$

$\Delta\omega_{\text{FWHM}}$ is the full-width at half-maximum. In the experimental part of our work, we have used optical filters with a variety of FWHM, from 0.4 to 0.8 nm with a central frequency of 1550 nm. The term $\delta\omega$ is the frequency deviation due to the time dependence phase shift (SPM) of the mode-locked pulse in the SOA. It is assumed that the filter maximum transmission is locked to the frequency peak of the mode-locked spectrum, which is $\omega - \delta\omega$.

2.2.2. Linear losses

The linear loss operator is defined as follows:

$$T_{\text{loss}} = \exp\left[-\frac{L}{2}\right] \tag{10}$$

where L is the losses in one round-trip, which is close to 6 dB.

2.2.3. Semiconductor optical amplifier

Finally, $\widehat{T}_2$ represents the amplitude and phase modulation at a frequency ω_{external} of the external pulses. In order to calculate operator $\widehat{T}_2$, the theory of short pulse propagation in SOAs is used [42,43]. SOAs have been extensively studied and modeled in the literature. However, a SOA acting as the gain modulator has not been yet modeled in a fiber ring laser configuration. In our approach, we have also included the phase change that the mode-locked pulse experience through its propagation from the nonlinear medium. This time dependent phase change result on a phase shift of the frequency. This is due to cross-phase modulation, induced by the externally introduced pulsed signal.

A simple and very successful model presented in [42] suffices to describe pulse propagation in a SOA. Starting from the carrier density (N) rate equation and neglecting carrier diffusion we reach a rate equation for the gain g,

$$g = \Gamma\alpha(N - N_0) \tag{11}$$

which is,

$$\frac{\partial g}{\partial t} = \frac{g_0 - g}{\tau_{\text{c}}} - \frac{g|A|^2}{E_{\text{sat}}} \tag{12}$$

where g_0 is the small signal gain defined by

$$g_0 = \Gamma a N_0\left(\frac{I}{I_0} - 1\right) \tag{13}$$

with

$$I_0 = \frac{qVN_0}{\tau_{\text{c}}} \tag{14}$$

In the above equations, various physical quantities enter. Their physical meaning together with the associated symbols is presented in Table 1.

$|A|^2 = p_{\text{in}}$ represents the power of the introduced pulsed signal. E_{sat} is the saturation energy above that it is assumed that the SOA is heavily saturated. The saturation energy is given by

$$E_{\text{sat}} = \frac{\hbar\omega_0\sigma}{a_{\text{int}}} \tag{15}$$

where α_{int} is the internal loss of the SOA. σ is the mode-cross-section area of the SOA given by

$$\sigma = \frac{wd}{\Gamma} \tag{16}$$

Introducing the function: $h(t) = \int_0^L g(z,t)\,\mathrm{d}z$ the rate equation for the integrated gain is

$$\frac{\mathrm{d}h}{\mathrm{d}t} = \frac{g_0 L - h}{\tau_{\text{c}}} - \frac{p_{\text{in}}(t)}{E_{\text{sat}}}\left[\mathrm{e}^{h(t)} - 1\right] \tag{17}$$

Table 1
Symbols of the various physical quantities of the ring laser model

Γ	the confinement factor
N_0	the carrier density required for transparency $= 0.9\times 10^{18}$ cm^{-3}
τ_c	the spontaneous carrier lifetime
q	the electron charge
V	the active volume of the SOA
I	the injection current and
α	the gain coefficient or line width enhancement factor

We have to solve the above ordinary differential equation (17) for $h(t)$ given P_{in}. Assuming that $\alpha_{\text{int}} \ll g$, the output power of the pulse is simply the input multiplied by the exponential of $h(t)$. We are interested to solve the above equation during the gain saturation regime and the gain recovery regime for both internal and external pulses.

2.2.3.1. Gain saturation. In this regime, we are neglecting carrier recovery during the pulse propagation due to current injection, i.e. width of the pulse smaller than the carrier lifetime of the amplifier. Eq. (17) is simplified as follows:

$$\frac{dh}{dt} = -\frac{p_{\text{in}}(t)}{E_{\text{sat}}}[e^{h(t)} - 1] \tag{18}$$

where $h_{\text{in}} = h(-\infty)$ and $U_{\text{in}} = \int_{-\infty}^{t} p_{\text{in}}(t)\,dt$ is the energy of the pulse contained in the leading part of the pulse up to t. Solving equation (18), we obtain:

$$h(t) = -\ln[1 - (1 - e^{-h_{\text{in}}})e^{-\frac{U_{\text{in}}(t)}{E_{\text{sat}}}}] \tag{19}$$

This function gives the integrated gain in the saturation regime. It will be used in the following part of the paper where the steady-state equations will be solved. It is worth noticing here, that in previous studies, authors either propose unnecessary preliminary expansions of the integrated gain into Taylor series, in terms of $\frac{U_{\text{in}}(t)}{E_{\text{sat}}} \leqslant 1$, or linearizations of the integrated gain that result in poor approximations. In what follows, a much more accurate method is presented in three steps. First Eq. (19) is solved and then for a certain pulse profile, U_{in} is calculated. It must be noted here that Eq. (19) has not been widely used in similar mode-locked laser models. Then the whole right hand side of Eq. (19) is expanded in terms of $t/\Delta T$ and finally the system of the steady-state equations is solved for mode-locking operation. This method differs from those proposed up to date in the literature and describes gain saturation accurately.

2.2.3.2. Gain recovery. After the saturation the SOA recovers due to carrier injection. We are assuming that the stimulated recombination is less important in this regime. Therefore, starting again from Eq. (17) the gain of the SOA recovers as follows:

$$\frac{dh}{dt} = \frac{g_0 L - h}{\tau_c} \tag{20}$$

which leads to the following expression:

$$h(t) = (h_f - h_s)e^{\frac{t}{\tau_c}} + h_s \tag{21}$$

with $h_s = g_0 L$ and $h_f = h(t = 0)$.

Small signal gain is usually expressed as follows: $G_s \equiv \exp(h_s/2)$. h_f is the integrated gain of the pulse immediately after the pulse transit that saturates the SOA. Therefore

$$h_f = -\ln[1 - (1 - e^{-h_{\text{in}}})e^{-u_0}] \tag{22}$$

where $U_0 = U_{\text{in}}(t = 0)/E_{\text{sat}}$ (U_0 is the normalized input pulse energy).

In our setup, two pulses are circulating in the ring, the external and the mode-locked pulses. T_s is the time difference between the centers of the two pulses. In our case, we are interested in solutions where T_s is larger than the width of the two pulses.

In order to obtain the steady-state condition for the laser oscillator, the gain of the SOA is assumed to recover always to the same level h_{in}^{p} and $h_{\text{in}}^{\text{ext}}$ before the mode-locked and the external pulses enter it, respectively. As the mode-locked pulse forms at time T_s after the external pulse has entered the SOA, its gain has had $T_s - \Delta T'$ time to recover to the value h_{in}^{p} from the value $h_{\text{in}}^{\text{ext}}$ before the arrival of the mode-locked pulse, where $\Delta T' \approx \frac{1}{2}(t_{\text{ext}} + t_{\text{p}})$, with t_{ext} being the FWHM of the external pulses and t_{p} the FWHM of the mode-locked pulses. Similarly, the external pulse experiences a gain equal to $h_{\text{in}}^{\text{ext}}$ which has recovered from the saturated value h_{f}^{p} after the mode-locked pulse exits the SOA after time $T_r - T_s - \Delta T'$ has elapsed (see Fig. 2).

The equation of the recovery of the SOA is thus separated in two equations which describe the SOA recovery after the transition of the external and mode-locked pulses, respectively. Eqs. (19) and (21) yield:

$$h_{\text{in}}^{\text{p}} = h_s + \left\{-\ln\left[1 - (1 - \exp(-h_{\text{in}}^{\text{ext}}))\exp\left(-\frac{U_{\text{in}}^{\text{ext}}(0)}{E_{\text{sat}}}\right)\right] - h_s\right\} \times \exp\left(-\frac{T_s - \Delta T'}{\tau_{\text{car}}}\right) \tag{23}$$

and

$$h_{\text{in}}^{\text{ext}} = h_s + \{-\ln[1 - (1 - \exp(-h_{\text{in}}^{\text{p}}))\exp(-U_0)] - h_s\} \times \exp\left(-\frac{T_r - T_s - \Delta T'}{\tau_{\text{car}}}\right) \tag{24}$$

By U_0 we denote the normalized pulse energy of the internal mode-locked pulse and by $U_{\text{in}}^{\text{ext}} \equiv U_{\text{in}}^{\text{ext}}(0)$ the energy of the externally introduced pulsed signal h_{in}^{p}. is an unknown parameter and depends on the U_0 and h_s. Solving the above system of equation we determine the unknown value of h_{in}^{p}.

3. Steady-state equation

In order to obtain the steady-state condition we assume that the pulse reproduces itself after each complete transit.

$$E_{\text{out}}(t) = E_{\text{pulse}}(t - T_R + \delta T)e^{+i\varphi} \tag{25}$$

with φ constant and δT the detuning between the modulating frequency and harmonic frequency of the cavity. Each time the pulse passes a medium the respective operator acts. Thus, we have:

$$E_{1\text{out}}(t) = \widehat{T_1}(t-t_1)E_{\text{pulse}}(t-t_1)$$
$$E_{2\text{out}}(t) = \widehat{T_2}(t-t_1-t_2)E_{1\text{out}}(t-t_2)$$
$$E_{3\text{out}}(t) = \widehat{T_3}E_{2\text{out}}(t)$$
$$E_{\text{out}}(t) = E_{3\text{out}}(t-t_3)$$

The above implies that

$$E_{\text{out}} = \widehat{T_3}\widehat{T_2}(t-T_R)\widehat{T_1}(t-T_{\text{R}})E_{\text{pulse}}(t-T_{\text{R}}) \tag{26}$$

Applying the $T_{\text{filter}}(\omega)$ operator on the transformed pulse in the frequency domain we find

$$T_{\text{filter}}(\omega)E_{\text{pulse}}(\omega) = \frac{k\Delta T}{\sqrt{1+\mathrm{i}\theta}}\mathrm{e}^{\frac{\delta T^2\omega^2}{1+\mathrm{i}\theta}}\mathrm{e}^{\frac{(\omega-\delta\omega)^2}{2\Delta\omega_{\text{g}}}} \tag{27}$$

The steady-state equation (25) can be evaluated now. Working in the time domain the steady-state equation takes a very complicated but compact form, that split to several equations needed to hold. However, we have first to insert the gain function into the steady-state equation. Based on Eq. (19), we evaluated the integrated gain for the certain pulse, we used in our model. We used up to second order terms which is a very good approximation and have not included in previous related studies [30,37]. Our approximation was checked and compared, for its validity, with the gain calculated numerically in other works [42]. This should be considered in addition to the complexity of our model stemming from the presence of the external modulating pulse. Thus, the following equations present the integrated gain to be included in the steady-state equations:

$$h(t) = \gamma + \delta t + \varepsilon t^2 \tag{28}$$

We obtain

$$\gamma = \frac{MU_0(4(M-1)\sqrt{2\pi}+\pi U_0) - 16(M-1)^2\ln(1-M)}{16(M-1)^2}$$
$$\delta = \frac{MU_0(-4+4M+\sqrt{2\pi}U_0)}{4(M-1)^2}$$
$$\varepsilon = \frac{MU_0^2}{2(M-1)^2} \tag{29}$$

where

$$M = 1-\exp(-h_{\text{in}}^{\text{p}}) \tag{30}$$

Using the above equations, we derive the equivalent system of six equations:

$$2\ln\left(\frac{\Delta T\Delta\omega_{\text{g}}}{\sqrt{r}}\right)\xi + 2\eta\theta + \frac{\delta T^2}{\Delta T^2}(\xi-\theta^2) - L\xi + \gamma\xi + 2\varphi\theta - \gamma\alpha\theta - \Delta\omega^2\Delta T^2 = 0 \tag{31}$$

$$\frac{2\delta T}{\Delta T^2}(\xi-\theta^2) + \frac{\delta\xi}{\Delta T} - \frac{\delta\alpha\theta}{\Delta T} + 2\Delta\omega\theta = 0 \tag{32}$$

$$\frac{\xi-\theta^2}{\Delta T^2} + \frac{\varepsilon\xi}{\Delta T^2} - \frac{\theta\alpha\varepsilon}{\Delta T^2} - \Delta\omega_{\text{g}}^2 = 0 \tag{33}$$

$$2\ln\left(\frac{\Delta T\Delta\omega_{\text{g}}}{\sqrt{r}}\right)\theta + 2\eta\xi + \frac{\delta T^2}{\Delta T^2}\theta(1+\xi) - L\theta - 2\varphi\xi + \alpha\xi\gamma + \gamma\theta = 0 \tag{34}$$

$$\frac{2\delta T}{\Delta T^2}(1+\xi)\theta + \frac{\alpha\xi\delta}{\Delta T} - 2\Delta\omega + \frac{\delta\theta}{\Delta T} = 0 \tag{35}$$

$$\frac{\theta(1+\xi)}{\Delta T^2} + \frac{\alpha\xi\varepsilon}{\Delta T^2} - \Delta\omega_{\text{g}}^2\theta + \frac{\varepsilon\theta}{\Delta T^2} = 0 \tag{36}$$

where

$$\eta = \frac{\arctan\left[\frac{\theta}{\xi}\right]}{2} \tag{37}$$
$$\xi = 1+\Delta T^2\Delta\omega_{\text{g}}^2 \tag{38}$$

and

$$r = \sqrt{\xi^2+\theta^2} \tag{39}$$

Unknown parameters in Eqs. (31)–(36) include. θ, ΔT, $\Delta\omega$, δT, U_0, ϕ. Performing complex calculations and observing some remarkable cancellations analytical solutions are derived:

$$\delta T = \frac{-\xi\delta(1+\alpha\theta)+\theta\delta(\alpha-\theta)}{2\Delta T\left(\Delta\omega_{\text{g}}^2(1+\theta)+\alpha\varepsilon(\theta-\xi)\frac{1}{\Delta T^2}-\varepsilon(\xi+\theta)\frac{1}{\Delta T^2}\right)} \tag{40}$$

$$\Delta\omega = \delta t\left(\Delta\omega_{\text{g}}^2\theta - \alpha\xi\varepsilon\frac{1}{\Delta T^2} - \varepsilon\theta\frac{1}{\Delta T^2}\right) + \frac{\alpha\xi\delta}{2\Delta T} + \frac{\delta\theta}{2\Delta T} \tag{41}$$

$$\theta = \frac{-\alpha\xi\varepsilon}{2+\varepsilon} \tag{42}$$

$$\Delta T = \frac{\sqrt{\rho-1}}{\Delta\omega_{\text{g}}} \tag{43}$$

$$\phi = -\eta + \delta T^2\Delta\omega_{\text{g}}^2\theta\frac{\xi-1}{2r^2} - \frac{\delta T^2}{2\Delta T^2}a\varepsilon + \frac{a\gamma}{2} + \Delta\omega^2\Delta T^2\frac{\theta}{2r^2} \tag{44}$$

where

$$\rho = \frac{-N+\sqrt{N^2+4\alpha^2(4+4\varepsilon+\varepsilon^2)}}{2\alpha^2\varepsilon} \tag{45}$$
$$N = -4-(2\alpha^2+4)\varepsilon-(\alpha^2+1)\varepsilon^2 \tag{46}$$

Note that η does not appear in the solutions.

Finally, the input pulse energy U_0 is evaluated solving the following equation:

$$2\ln\left[\frac{\Delta T\Delta\omega_{\text{g}}}{\sqrt{r}}\right]r^2 + \delta T^2\left(\Delta\omega_{\text{g}}^2+\frac{\theta\alpha\varepsilon-\varepsilon\xi}{\Delta T^2}\right)\xi + \delta T^2(\Delta\omega_{\text{g}}^2\theta+\frac{-\xi\alpha\varepsilon-\varepsilon\theta}{\Delta T^2})\theta - Lr^2 + \gamma r^2 - \Delta\omega^2\Delta T^2\xi = 0 \tag{47}$$

The above formulae epitomize the analytically solved mode locking conditions we have to know in order to study the presented laser model.

4. Results and discussion

In this section, the effect of certain critical variables on the behavior of the SOA-based fiber ring laser is presented. The pulsewidth of the mode-locked pulse is given by Eq.

(43). The pulsewidth depends on $\Delta\omega_g$ (Eq. (43)), α (Eqs. (45) and (46)) and h_{in}^{p} (Eqs. (29) and (30)). h_{in}^{p} is the gain that the mode-locked pulse experiences before entering the SOA and depends on U_{in}^{ext}, T_s, t_{ext}, the external pulse period T_{ext}^{period} (through T_r) as well as on the SOA related parameters i.e. τ_{car}, E_{sat}, g_0, L via Eqs. (23) and (24). From the above parameters only T_s is regarded as an unknown parameter, while the rest are external inputs to the system. The parameters we used in the calculations are shown in Table 2.

The above-mentioned SOA values correspond to those used in the experiment [28–34] and refer to a 500-μm bulk InGaAsP–InP ridge waveguide SOA with 10 angled and antireflection coated facets. The SOA had a peak gain at 1535 nm with 20-nm bandwidth, providing 23-dB small signal gain with 250-mA dc drive current and had 400-ps recovery time.

Using the above parameters, we investigated two regions of operations. One finely tuned region by setting $\delta T = 0$ and one slightly detuned for $\delta T = 0.2$ ps. The model developed revealed a remarkable interrelated condition of the SOA gain and the energy of the externally introduced signal -locus of G_s, U_{in}^{ext} parameters. This had been verified experimentally, in the results presented in [28–34]. In particular, it was found that stable mode-locked operation could be achieved for a range of SOA gains in a monotonic combination with the energy of the externally introduced optical signal. Most theoretical studies on SOA-based ring laser presume a constant SOA gain as well as a constant carrier lifetime. However, both parameters changes dramatically with the SOA driving current. In our analysis, we employed two set of parameters as shown in Table 2.

In what follows, we present results for the tuning regime that is when $\delta T = 0$ and for the slightly detuning regime when $\delta T = 0.2$ ps.

4.1. Tuning regime

Setting $\delta T = 0$, we are able to find the region of the input parameters that ensure mode locking operation and minimum mode-locked pulse. In our model, a worth mentioning result is the fact that in this perfectly tuned case Eqs. (41)–(44) and (47) suffice to determine the desired quantities that characterize the mode-locked system θ, ΔT, $\Delta\omega$, U_0, ϕ, while the condition of $\delta T = 0$ determines h_{in}^{p} as well. This consequently determines, through Eqs. (23) and (24), the locus of points G_s, U_{in}^{ext} that ensure $\delta T = 0$. Figs. 3 and 4 show the locus of G_s, U_{in}^{ext} parameters to achieve perfect mode-locking for τ_{car} values of 800 and 400 ps, respectively. Both figures were drawn for $\Delta\omega g = 0.36$ nm and $\alpha = 4$ that provide $h_{in}^{p} = 3.89$, $U_0 = 0.032$ fJ and $\Delta T = 13.344$ ps (for ΔT, see Eq. (1)).

From both of the above figures, it can be seen that for perfect mode-locking an increase in the external power must be always accompanied with an increase in the SOA gain, that means an increase in its driving current. With respect to Fig. 4, exact tuning takes place for a shorter range of values, since it must be ensured that T_s is larger than the width of the internal and the external pulses.

Figs. 5–7 show the effect of filter bandwidth in the system. In particular, Figs. 5 and 6 show the effect on the pulsewidth and energy of the mode-locked pulse, while Fig. 7 shows the effect on pulse chirp parameter, θ. The first points of these figures accounts for $\Delta\omega g = 0.36$ nm, $\Delta T = 13.344$ ps, $U_0 = 0.032$ fJ and $\theta = -5.7$, and which

Table 2
Set of values used in the calculations

Carrier lifetime, τ_c	400 ps at $I_{SOA} = 120$ mA 800 ps at $I_{SOA} = 250$ mA
Small signal gain	23 dB at $I_{SOA} = 250$ mA 17 dB at $I_{SOA} = 120$ mA
Cavity length	10.5 m
External pulse period	100 ps
External pulse energy	100–200 fJ at 10 GHz
Pulsewidth of external pulses	7 ps
SOA saturation energy, E_{sat}	2000 fJ
Gain coefficient, α	4
Cavity loss, L	4 dB

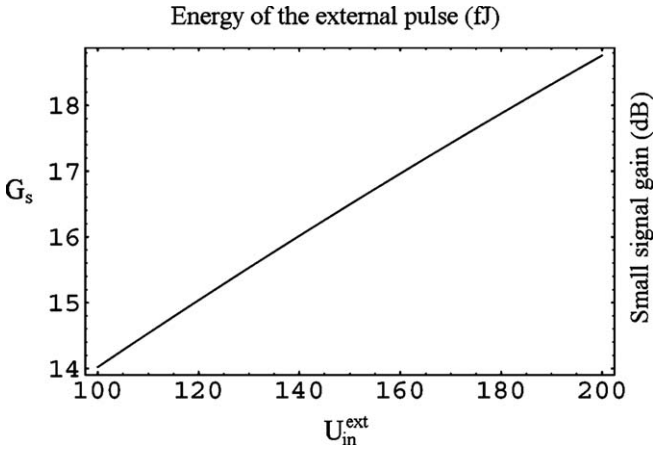

Fig. 3. Locus of U_{in}^{ext}, G_s points for exact mode-locking and for $t_{car} =$ 800 ps.

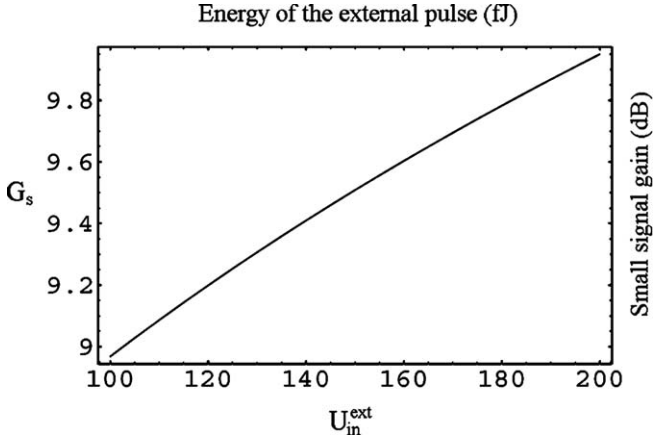

Fig. 4. Locus of U_{in}^{ext}, G_s points for exact mode-locking and for $t_{car} =$ 400 ps.

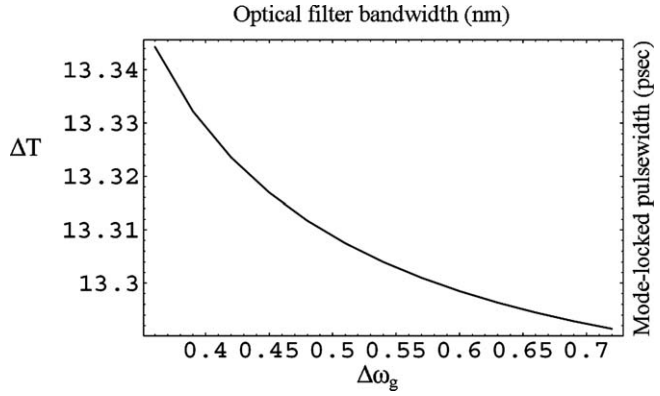

Fig. 5. Effect of optical filter bandwidth on the mode-locked pulse width.

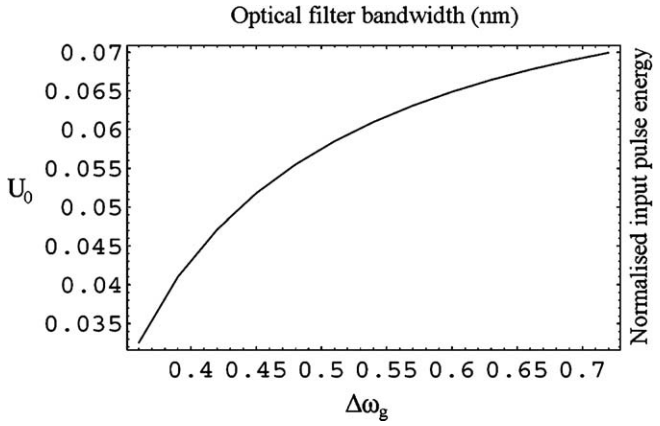

Fig. 6. Effect of optical filter bandwidth on the mode-locked pulse energy.

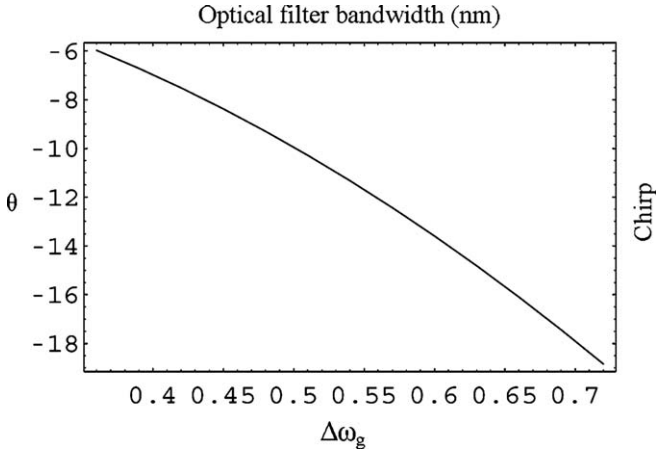

Fig. 7. Effect of optical filter bandwidth on the chirp of the mode-locked pulses.

are associated to all points of the locus illustrated in Figs. 3 and 4, though with different T_s values. In other words all the pairs of G_s, U_{in}^{ext} on the curves shown in Figs. 3 and 4 provide $U_0 = 0.032$ fJ, $\theta = -5.7$ and $\Delta T = 13.344$ ps (note that $\alpha = 4$, $h_{in}^{p} = 3.89$). The rest of the points in Figs. 5–7 correspond to different families (other values of h_{in}^{p}) of curves of exact mode locking.

From the above figures, it can be seen that the broader the filter is, the shorter the pulsewidth and the higher the energy of the mode-locked pulse. However, this come with a certain limit that stems from the locus range of h_s, U_{in}^{ext}. Further, the broader filter causes an increase on the chirp (see Fig. 7) due to the new red-shifted components created in the recirculation. It must be noted here that the nonlinear terms of the gain function allow the appearance of significant non-zero values of the chirp parameter that cannot be neglected. Clearly, a linear approximation of the gain would result to zero chirp when dispersion is not included [36]. This is an important outcome of our study that needs to be taken under consideration in future theoretical model constructions.

Finally for this regime of operation, we have also investigated the effect of the gain coefficient or so called SOA linewidth enhancement factor, α. Our model revealed that a steady-state solution, across the locus of h_s, U_{in}^{ext} can be provided for α values in the range of $3.8 < \alpha < 4.2$. Within this range, ΔT, U_0 vary but not significantly, while chirp increases when α gets larger. Fig. 8 shows chirp variation. It can be seen that as the gain coefficient factor gets larger, a rise on the shift between the center of the mode-locked pulses and the filter occurs, that results in the augmentation of the SPM induced chirp. It is evident that for obtaining a low chirp value, a small gain coefficient must be chosen.

4.2. Detuning regime

In this section, results concerning the slightly detuned regime of operation are presented. In general, a laser system may exhibit a very different behavior when it is tuned away its optimum values. In our case, it is interested to study the performance of the laser when its cavity frequency is detuned away from being an integer multiple of the external pulsetrain frequency. Our general approach of solving the steady-state equations, keeping a non-zero $\delta T \neq 0$ term in Eq. (25), makes calculations complicated, but however, allows the study of this interesting regime To this end, we have set $\delta T = 0.2$ ps and investigated again the locus of U_{in}^{ext}, G_s as well as the effect of filter bandwidth

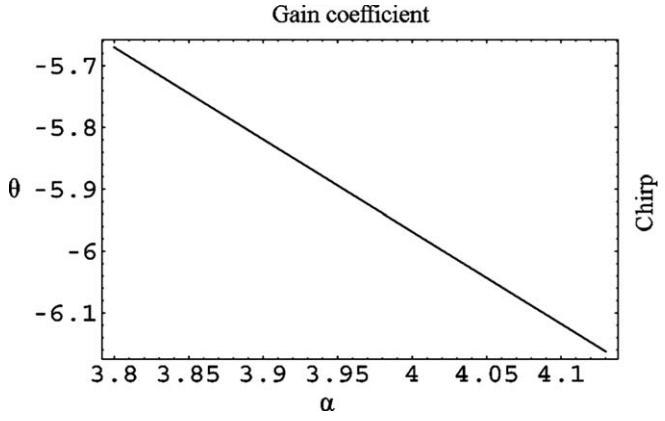

Fig. 8. Effect of gain coefficient α on the pulse chirp.

and gain coefficient. Regarding the effect of the gain coefficient, α, it was similar with that of the exact tuned regime of operation but with a slight variation on the mode-locked pulse duration and pulse. Fig. 9 shows the locus of points for $t_{car} = 400$ ps. As expected the locus curve resembles the tuned case shown in Fig. 4, but in this case a higher gain is needed. Results shown correspond to $\Delta\omega g = 0.36$ nm and $\alpha = 4$ that provide $h_{in}^{p} = 4.11$.

Figs. 10 and 11 show the effect of filter bandwidth on the mode-locked pulsewidth and energy, while Fig. 12 shows the effect on the mode-locked pulse chirp. The first points of Figs. 10–12, ($\Delta\omega g = 0.36$ nm) are associated to all the points of the curve in Fig. 9, with different T_s though, while the rest of the points correspond to different families (other values of h_{in}^{p}) of curves of the detuned regime. It must be noted here that results shown in Figs. 5 and 10 are not directly comparable since they correspond to different values of h_{in}^{p} and T_s. From Figs. 10 and 11, it can be noted the different behavior of ΔT and U_0 with respect to $\Delta\omega g$. It is evident that the increase of the filter bandwidth results in unstable operation. The overall unstable performance can be explained from the fact that the locking bandwidth in this regime of operation is significantly smaller. The locking bandwidth is defined as the bandwidth around the external f_{ext} frequency within which mode-locked operation can be obtained without a pulsetrain loss. Increasing the optical filter bandwidth results in the oscillation of other optical frequencies in CW mode.

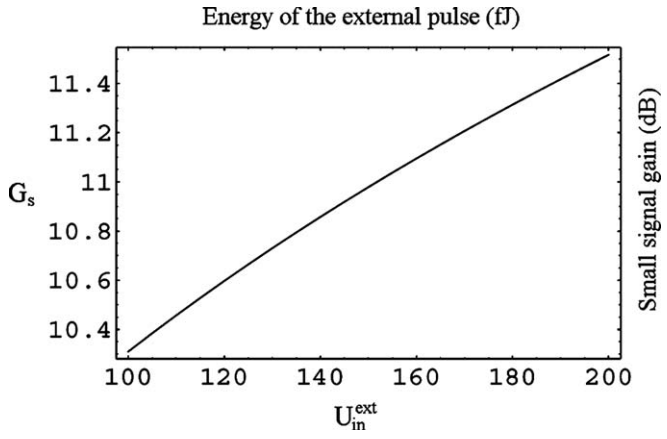

Fig. 9. Locus of U_{in}^{ext}, G_s points for the slightly detuned regime of operation and for $t_{car} = 400$ ps.

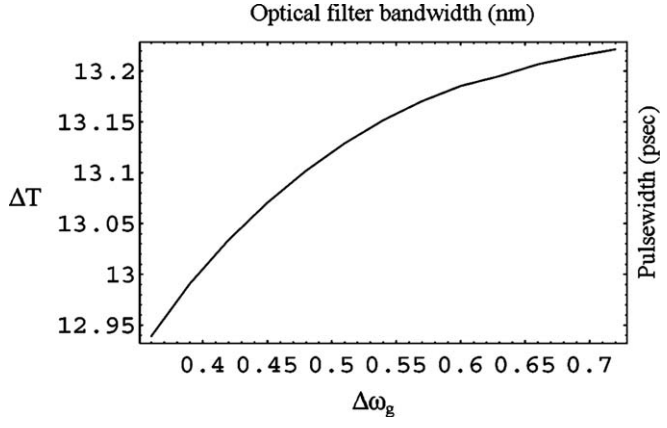

Fig. 10. Effect of optical filter bandwidth on the pulsewidth of the slightly detuning regime ($\delta T = 0.2$ ps).

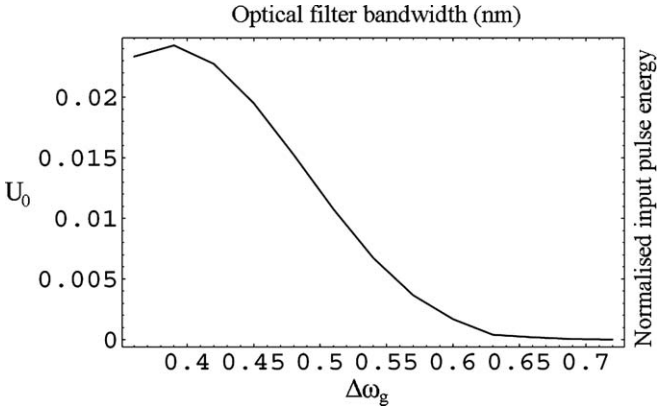

Fig. 11. Effect of optical filter bandwidth on the energy of the slightly detuning regime ($\delta T = 0.2$ ps).

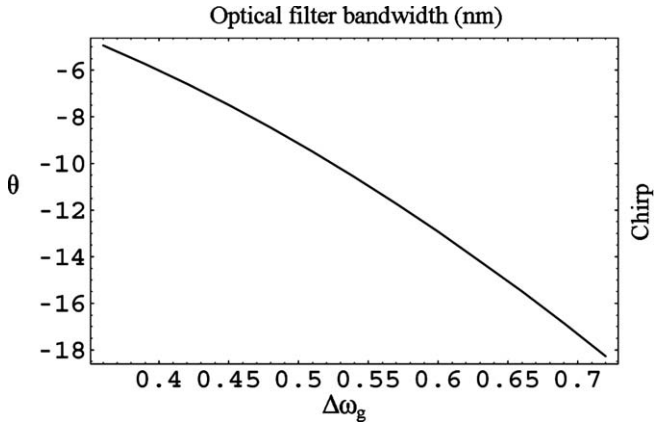

Fig. 12. Effect of filter bandwidth on the chirp ($\delta T = 0.2$ ps).

5. Conclusions

In this paper, a self-consistent model of a SOA-based ring laser was presented. The laser uses an intra-cavity semiconductor optical amplifier (SOA) for signal amplification as well as for gain modulation. Gain modulation is achieved with the introduction of an external optical pulsetrain. The model developed was solved analytically and revealed the locus of G_s, U_{in}^{ext} parameters for a tuned and a slightly detuned mode of operation. In our analysis, we have assumed SOA-gain saturation by both the external and mode-locked pulsetrains, and no linear expansion of SOA gain profile, resulting in a complex but accurate theoretical model. Using this model, we have investigated the effect of the filter bandwidth and the gain coefficient on the mode-locked pulsewidth and energy as well as on

the pulse chirp. It was found that pulsewidth and energy decreases/increases respectively with the filter bandwidth, while chirp increases as well, due to the new red-shifted components created in the recirculation. Furthermore, in this paper, we have also investigated, a slightly detuned mode of operation, when cavity frequency is slightly tuned away from the external pulse frequency. The study of this regime revealed some new interesting features, and particularly it was found that pulsewidth and energy of the mode-locked pulse drops fast with the increase of the filter bandwidth. To this end, we may assume that mode-locking in this regime is unstable and may result in pulse drop outs.

The presented analytical solutions can be used for any similar SOA-based ring laser setup due to the generic approach followed.

References

[1] E.A. Swanson, S.R. Chinn, K. Hall, K.A. Rauschenbach, R.S. Bondurant, J.W. Miller, IEEE Photon. Technol. Lett. 6 (10) (1994) 1194.
[2] K. Sato et al., Electron. Lett. 34 (8) (1998) 790.
[3] S. Arahira, Y. Ogawa, Electron. Lett. 37 (16) (2001) 1026.
[4] H.A. Haus, J. Appl. Phys. 51 (1980) 4042.
[5] L.A. Zenteno, H. Avramopoulos, G.H.C. New, Appl. Phys. B 40 (3) (1986) 141.
[6] G.T. Harvey, Linn F. Mollenauer, Opt. Lett. 18 (2) (1993) 107.
[7] A.D. Ellis, R.J. Manning, I.D. Phillips, D. Nesset, Electron. Lett. 35 (8) (1999) 645.
[8] L. Duan, C. Richardson, Z. Hu, M. Dagenais, J. Goldhar, IEEE Phot. Technol. Lett. 14 (6) (2002) 840.
[9] J. Roth, K. Dreyer, B. Collings, W. Knox, K. Bergman, IEEE Photon. Technol. Lett. 14 (7) (2002) 917.
[10] G.E. Town, L. Chen, P.W.E. Smith, IEEE Phot. Technol. Lett. 12 (11) (2000) 1459.
[11] A. Bellemare et al., IEEE J. Select. Top. Quantum Electron. 7 (1) (2001) 22.
[12] M. Horowitz, C. Menyuk, T. Carruthers, Irl N. Duling III, IEEE J. Light. Technol. 18 (11) (2000) 1565.
[13] H. Takara, S. Kawanishi, M. Sarawatari, K. Noguchi, Electron. Lett. 28 (22) (1992) 2095.
[14] M. Nakazawa, E. Yoshida, Y. Kimura, Electron. Lett. 30 (19) (1994) 1603.
[15] Th. Pfeiffer, G. Veith, Electron. Lett. 29 (1993) 1849.
[16] Chung Ghiu Lee, Yun Jong Kim, Hyoung Kyu Choi, Chang-Soo Park, Opt. Commun. 209 (2002) 417.
[17] X. Shan, T. Woddowson, A.D. Ellis, A.S. Siddiqui, Electron. Lett. 32 (11) (1996) 1015.
[18] E. Yoshida, M. Nakazawa, Electron. Lett. 34 (18) (1998) 1753.
[19] H. Takara, S. Kawanishi, M. Sarawatari, Electron. Lett. 31 (4) (1995) 292.
[20] K. Gupta, N. Onodera, K. Abedin, M. Hyodo, IEEE Photon. Technol. Lett. 14 (3) (2002) 284.
[21] C. Depriest, T. Yilmaz, S. Etamad, A. Braun, J. Abeles, P. Delfyett, in: Optical Fiber Communication Conference and Exhibit, 2002, p. 589.
[22] X. Lei, B.C. Wang, V. Baby, I. Glesk, P.R. Prucnal, in: 14th Annual Meeting of the IEEE/LEOS, vol. 2, 2001, p. 421.
[23] M.J. Guy, J.R. Taylor, D.G. Moodie, A.E. Kelly, Electron. Lett. 32 (24) (1996) 2240.
[24] C. Peng, M. Yao, J. Zhang, H. Zhang, Q. Xu, Y. Gao, Opt. Commun. 209 (2002) 181.
[25] H. Shi, G.A. Alphonse, J.C. Connolly, P.J. Delfyett, Electron. Lett. 34 (2) (1998) 179.
[26] D.M. Patrick, Electron. Lett. 30(1) 43.
[27] K.L. Hall, J.D. Moores, K.A. Rauschenbach, W.S. Wong, E.P. Ippen, H.A. Haus, IEEE Photon. Technol. Lett. 7 (9) (1995) 1093.
[28] T. Papakyriakopoulos, A. Hatziefremidis, T. Houbavlis, H. Avramopoulos, in: Optical Fiber Communication Conference, vol. 1, 1999, p. 4.
[29] K. Vlachos, Chris Bintjas, Nikos Pleros, Hercules Avramopoulos, IEEE J. Select. Top. Quantum Electron. 10 (1) (2004) 147.
[30] K. Zoiros, K. Vlachos, T. Stathopoulos, C. Bintjas, H. Avramopoulos, in: Optical Fiber Communication Conference, vol. 1, 2000, p. 256.
[31] K. Vlachos, K. Zoiros, T. Houbavlis, H. Avramopoulos, IEEE Photon. Technol. Lett. 12 (2) (2000) 214.
[32] K. Vlachos, H. Avramopoulos, SPIE J. Opt. Eng. 42 (2) (2003) 300.
[33] K. Vlachos, T. Koonen, G. Theophilopoulos, H. Avramopoulos, J. Opt. Quantum Electron. 35 (9) (2003) 865.
[34] K. Vlachos, Elsevier J. Opt. Commun. 222 (2003) 249.
[35] K. Zoiros et al., Opt. Commun. 180 (2000) 301.
[36] C. Peng, M.Y. Yao, J.F. Zhang, Opt. Commun. 209 (2002) 181.
[37] K.E. Zoiros, T. Houbavlis, M. Moyssidis, Opt. Commun. 254 (4–6) (2005) 310.
[38] D.J. Kuizenga, A.E. Siegman, IEEE J. Quantum Electron. 6 (1970) 694.
[39] A.E. Siegman, Lasers, University Science Books, Mill Valley, CA, 1986.
[40] H.A. Haus, Waves and Fields in Optoelectronics, Prentice Hall, New Jersey, 1984.
[41] H.A. Haus, Compact Sources of Ultra-short Pulses, Cambridge University Press, Cambridge, UK, 1995 (Chapter 1).
[42] G. Agrawal, N.A. Olsson, J. Quantum Electron. 25 (11) (1989) 2297.
[43] M. Eiselt, W. Pieper, H.G. Weber, IEEE/OSA J. Lightwave Technol. 13 (10) (1995) 2099.